



ALMA MATER STUDIORUM
UNIVERSITÀ DI BOLOGNA

ARCHIVIO ISTITUZIONALE
DELLA RICERCA

Alma Mater Studiorum Università di Bologna Archivio istituzionale della ricerca

Testing the impact of discoplasty on the biomechanics of the intervertebral disc with simulated degeneration:
An in vitro study

This is the final peer-reviewed author's accepted manuscript (postprint) of the following publication:

Published Version:

Techens C., Palanca M., Eltes P.E., Lazary A., Cristofolini L. (2020). Testing the impact of discoplasty on the biomechanics of the intervertebral disc with simulated degeneration: An in vitro study. *MEDICAL ENGINEERING & PHYSICS*, 84, 51-59 [10.1016/j.medengphy.2020.07.024].

Availability:

This version is available at: <https://hdl.handle.net/11585/808871> since: 2021-02-27

Published:

DOI: <http://doi.org/10.1016/j.medengphy.2020.07.024>

Terms of use:

Some rights reserved. The terms and conditions for the reuse of this version of the manuscript are specified in the publishing policy. For all terms of use and more information see the publisher's website.

This item was downloaded from IRIS Università di Bologna (<https://cris.unibo.it/>).
When citing, please refer to the published version.

(Article begins on next page)

This is the final peer-reviewed accepted manuscript of:

**Med Eng Phys. 2020 Oct;84:51-59. doi:
10.1016/j.medengphy.2020.07.024. Epub 2020 Jul 30.**

**Testing the impact of discoplasty on the biomechanics of the
intervertebral disc with simulated degeneration: An in vitro study**

Chloé Techens, Marco Palanca, Peter Endre Éltés, Áron Lazáry, Luca
Cristofolini

PMID: 32977922 DOI: 10.1016/j.medengphy.2020.07.024

The final published version is available online at:

<https://doi.org/10.1016/j.medengphy.2020.07.024>

Rights / License:

The terms and conditions for the reuse of this version of the manuscript are specified in the publishing policy. For all terms of use and more information see the publisher's website.

Testing the impact of discoplasty on the biomechanics of the intervertebral disc with simulated degeneration: an *in vitro* porcine study

Chloé Techens, MEng¹, Marco Palanca, Ph.D.¹, Peter Endre Eltes MD²,
Aron Lazary PhD², Luca Cristofolini, Ph.D.¹

¹ Department of Industrial Engineering, School of Engineering and Architecture, Alma Mater Studiorum - Università di Bologna, Bologna, Italy

² R&D Department of National Center for Spinal Disorders, Budapest, Hungary

***Submitted to:* Medical Engineering & Physics, special issue “Biomechanics for in silico clinical trials: thematic symposium of the IX Meeting of the Italian Chapter of the European Society of Biomechanics”**

Original submission: 4th March 2020

Revised version: 18th July 2020

Statistics:

Word count (manuscript):	@ 4890 words
Word count (abstract):	@ 238 words
Figures:	@ 9
Tables:	@ 2
References:	@ 43

Corresponding author:

Luca Cristofolini
Department of Industrial Engineering
School of Engineering and Architecture
University of Bologna
Viale Risorgimento, 2
40136 Bologna, Italy
e-mail: luca.cristofolini@unibo.it

1 **ABSTRACT**

2 Percutaneous Cement Discoplasty has recently been developed to relieve pain in highly
3 degenerated intervertebral discs presenting a vacuum phenomenon in patients that
4 cannot undergo major surgery. Little is currently known about the biomechanical effects
5 of discoplasty. This study aimed at investigating the feasibility of modelling empty discs
6 and subsequent discoplasty surgery and measuring their impact over the specimen
7 geometry and mechanical behavior. Ten porcine lumbar spine segments were tested in
8 flexion, extension, and lateral bending under 5.4 Nm (with a 200 N compressive force
9 and a 27 mm offset). Tests were performed in three conditions for each specimen: with
10 intact disc, after nucleotomy and after discoplasty. A 3D Digital Image Correlation
11 (DIC) system was used to measure the surface displacements and strains. The posterior
12 disc height, range of motion (ROM), and stiffness were measured at the peak load. CT
13 scans were performed to confirm that the cement distribution was acceptable.
14 Discoplasty recovered the height loss caused by nucleotomy ($p=0.04$) with respect to
15 the intact condition, but it did not impact significantly either the ROM or the stiffness.
16 The strains over the disc surface increased after nucleotomy, while discoplasty
17 concentrated the strains on the endplates. In conclusion, this preliminary study has
18 shown that discoplasty recovered the intervertebral posterior height, opening the
19 neuroforamen as clinically observed, but it did not influence the spine mobility or
20 stiffness. This study confirms that this *in vitro* approach can be used to investigate
21 discoplasty.

22 **Keywords:**

23 Percutaneous Cement Discoplasty, Spine, Biomechanical testing, Strain

24 1. INTRODUCTION

25 Intervertebral Disc (IVD) degeneration is one of the main causes of low back pain, a
26 large socio-economic burden for society, affecting between 60% and 70% of the
27 population in industrialized countries at least once during their lifetimes [1]. Interbody
28 fusion with the insertion of an intervertebral spacer after performing disc fenestration is
29 the most common surgical treatment and has been widely studied in the literature [2]–
30 [10]. It requires an invasive surgery which lasts for hours and is often associated with
31 significant blood loss, long recovery, and general anaesthesia which is not suitable for
32 elderly patients or those with significant comorbidities. Since this disease appears with
33 age, finding minimally invasive treatments is crucial to treat the most complex cases.
34 Percutaneous Cement Discoplasty (PCD), a surgical technique that minimizes the
35 surgical morbidity and complication risks, is applied when a vacuum phenomenon is
36 observed inside the IVD, resulting in the collapse of the adjacent vertebra and in nerve
37 root compression. It consists of injecting an polymethylmethacrylate cement (PMMA)
38 to “create individually shaped “in-site” intervertebral spacers” in order to recover the
39 disc height and decompress the spinal canal [11]. One advantage of using PMMA to
40 stabilize the spine is that “the load-bearing surface of the implant is fully adapted to the
41 shape of the endplates”.

42

43 PCD is a newly developed technique, the authors found very little literature on the
44 subject. Varga *et al* presented in 2015 the technique and their clinical study on 47
45 patients showed significant improvement in their quality of life, correlating with a pain
46 factor decrease at 6 month follow-up [11]. Another study reported the surgery of a
47 patient treated with PCD [12]. Discoplasty was shown to positively affect the spinal
48 alignment and neuro-foraminal height in 27 patients [13].

49 While the impact of PCD on spine has been clinically assessed by comparing pre-
50 operative/post-operative scores, no indication about spine kinetics and kinematics has
51 been found by the authors. Some studies investigated similar techniques on animals,
52 performing *in vitro* testing of spines in intact condition (with a full IVD), after removal
53 of the Nucleus Pulposus (NP), and/or after a stabilization surgery. Refilling of the disc
54 with soft materials [14] to recover intact spine mechanics was also investigated,

55 however it differs from discoplasty which uses acrylic cement. Only Moissonier *et al*
56 and Wilke *et al* mimicked the PCD technique, implanting a spacer within the empty disc.
57 The first demonstrated that nucleotomy of canine IVD increased the Range of Motion
58 (ROM) and reduced disc height, whereas the presence of a hard mass inside the disc
59 recovered the height loss but left ROM as wide as after nucleotomy [3]. The second
60 attested that bone cement stabilized cervical discs, reducing the ROM compared to an
61 intact spine [15]. Moreover, using animal surrogates usually limits access to naturally
62 degenerated discs, consequently research has also focused on the best technique to
63 model the vacuum phenomenon [16], [17], and the mechanical consequences of that
64 surgery [18], [19]. In conclusion, PCD surgery relies on a weak knowledge of the
65 mechanics of lumbar spine treated this way.

66 This study aims at enlarging knowledge about the mechanical consequences of PCD on
67 lumbar spine stability. The motivations were two-fold: first, to develop a method to
68 artificially represent a vacuum disc and the surgical technique applied to *in vitro*
69 specimens, and to check the efficiency of this method as a model of PCD. Secondly, the
70 study aimed at developing a methodology assessing the biomechanics of the spine before
71 and after discoplasty. In particular, we hypothesized that PCD would recover the
72 posterior disc height, affect the mechanical behaviour of the spine and present a damage
73 risk for the surrounding tissue due to cement presence.

74 **2. MATERIALS AND METHODS**

75 **2.1. Specimens**

76 Ten functional spinal units were transected between T13 and L6 from porcine (*sus scrofa*
77 *domesticus*) thoracolumbar spines. The animals were young and healthy porcine
78 (approximately 9 months old and 100 kg) sacrificed for alimentary purposes. The
79 specimens were cleaned using surgical tools: all soft tissues were carefully removed
80 from the segment without damaging the vertebra, the facet joints and the intervertebral
81 disc. In order to keep the natural kinetics of the segment while testing, the anterior,
82 supraspinous and posterior ligaments were left intact. Each segment was aligned based
83 on the disc orientation, using a six-degree-of-freedom clamp. Both segment extremities
84 were potted with acrylic bone cement. Specimens were stored frozen at -20 °C between
85 cleaning and testing phases and between the tests which has been proven not to affect
86 significantly the segment biomechanics [20].

87 **2.2. Surgical procedure**

88 The purpose of the study is to develop a method to investigate the impact of PCD on the
89 biomechanical behaviour of the spine by comparing IVD treated by this technique to
90 degenerated and healthy IVDs. Thus, each specimen was tested in the three conditions
91 sequentially:

- 92 • intact (INT) with a healthy IVD,
- 93 • after nucleotomy (NUCL) to simulate the instability of degenerated discs,
- 94 • after discoplasty (DP) (Fig. 1).

95 **2.3. Nucleotomy**

96 Since the porcine specimens were euthanized before reaching skeletal maturation,
97 degenerated disc instability has been manually simulated by reproducing the vacuum
98 inside of the disc. The specimens were thawed at room temperature. A square incision
99 was performed with a scalpel blade in the annulus fibrosus on the latero-posterior side
100 of the disc. The nucleus pulposus, easily identified due to its softness, was completely
101 extracted through the excision with a curette. The endplates were shaved by scratching
102 off the soft tissue until the surfaces felt smooth. This did not weaken the endplates, as
103 no intravertebral leakage was observed during discoplasty. The size of the incision
104 corresponded to the disc height. The specimens were frozen at -20 °C until testing.

105 **2.4. Discoplasty**

106 After being tested in degenerated conditions, the specimens were treated with
107 discoplasty. For that, the specimens were thawed at room temperature. A high-viscosity
108 radiopaque acrylic bone cement (10% BaSO₄) (Tecres, Italy) was injected inside the
109 disc through the incision. Because the empty IVD was no longer in tension, the segment
110 was distracted/stretched during the injection to avoid an underestimation of the cement
111 volume. After injection, the cement hardened for 30 min. The specimens were frozen at
112 -20 °C until testing. In one specimen the facet joint was unintentionally damaged at the
113 end of the last test: checking the test results in retrospect confirmed there was no artefact.

114 **2.5. Mechanical testing**

115 All the specimens underwent the same test conditions. In order to simulate *in vivo*
116 kinetics of porcine spines, a load with offset was applied to simulate flexion, extension,

117 and lateral bending (the same side was selected for each specimen based on the possible
118 damages made during the preparation). This simplified loading scenario was chosen as
119 it allows reproducible simulation of a realistic loading scenario. In quadrupeds, the
120 choice of a side is less significant than for humans since they do not have a predisposed
121 limb side. The specimens were mechanically tested with a uniaxial servo-hydraulic
122 testing machine (Mod. 8032, Instron, UK) operated in displacement control. The upper
123 pot was rigidly fixed to the top of the testing machine while the other was loaded through
124 a spherical joint moving along a rail (Fig. 1). Before testing, each specimen was thawed
125 at room temperature and pre-conditioned applying a sinusoidal loading at 0.5 Hz for 20
126 cycles to minimize viscoelastic creep effect. Specimens were loaded at 5.4 Nm by
127 applying 200 N with an offset of 27 mm. The loading ramp lasted 1 s then the maximum
128 loading was maintained for 0.3 s and the specimen was unloaded. The cycle was
129 repeated 6 times (Fig. 2). Three cycles were found to be sufficient for preconditioning
130 the data in another study [21], further cycles being nearly identical. The same trend was
131 observed in these tests. The loading conditions were selected within the range of
132 biological conditions, similar to other past studies [7], [14], [22]–[25]. Besides, the
133 selected load avoided specimen damage. Each test was repeated twice to prove the
134 experiment repeatability. Data extracted from the last cycle of both runs were averaged
135 for each specimen. Axial load and displacement were acquired by the DIC system
136 connected to a load cell (100 kN) at 15 Hz. Additionally, to have a more reliable
137 sequence, the data were recorded with an independent computational unit (PXI,
138 Labview, National Instruments, Aus. Texas, US) at 500 Hz. Unfortunately, some of the
139 former records were missing for the first tests. Loads were either interpolated to have
140 more data or smoothed with a median filter depending of the acquisition frequency.

141 **2.6. Displacement and strain with DIC**

142 For each test, the specimen surface has been studied using a Digital Image Correlation
143 set-up in order to track its displacements and strains. This technique requires a high-
144 contrast speckle pattern on the region of interest. Thus, a white-on-black speckle pattern
145 was prepared on both the vertebra and the intervertebral disc (Fig. 1). First, the segment
146 was stained 3 times with a methylene blue solution to create a dark background without
147 impacting the properties of the tissues [26]. The white pattern was then sprayed
148 following a procedure optimized elsewhere [27]. To measure the displacements and the
149 deformations over the specimen surface, a 3D-DIC system (Q400, Dantec Dynamics,

150 Skovlunde, Denmark) and the associated software (Instron 4D, v.4.3.1, Dantec
151 Dynamics) were used. Images were acquired by two cameras (5 Megapixels, 2440 x
152 2050 pixels, 8-bit) with high-quality 35 mm lenses (Apo-Xenoplan 1.8/35, Schneider-
153 Kreuznach, Bad-Kreuznach, Germany) inclined at an angle of 26° (white dot line on
154 Fig. 1). The field of view covered the entire specimen (about 50mm by 30mm), which
155 gave a pixel size of about 0.02mm. The specimen was lit by cold-light LEDs. Before the
156 tests, calibration of the DIC system was performed using a dedicated target (A14-BMB-
157 9x9, Dantec Dynamics). The parameters for the images acquisition and the correlation
158 analysis have been previously optimized to minimize the error: facet size of 35 pixels,
159 grid spacing of 11 pixels, and local filtering with a 7x7 pixels kernel. In order to
160 investigate the biomechanical behaviour of the spine, two different acquisitions were
161 performed:

- 162 • For extension and flexion: Lateral view of the segment with the cameras pointing
163 at the neuroforamen
- 164 • For lateral bending; Frontal view of the specimen with the cameras pointing to
165 the selected bending side

166 Images were taken at 15 Hz from the unloaded condition (reference frame, no load
167 applied) to the end of the 6th cycle.

168 **2.7. Data analysis and statistics**

169 The parameters were extracted from the last load cycle of each of the two repetitions of
170 each loading configuration. All measurements were compared for each specimen
171 between the three disc conditions: intact, nucleotomy, discolplasty. In order to assess the
172 changes in the nerve space in the neuroforamen, which is the main point in doing
173 discolplasty, the posterior disc height was measured using DIC images: one point on each
174 endplate was identified on the 3D profile of the disc in the back of the disc, close to the
175 neuroforamen, where the nerve is passing. The points were aligned in the cranial-caudal
176 direction. Their position was therefore tracked using DIC software. As a result, posterior
177 disc height was only computed in flexion and extension, the frontal view not allowing
178 height computation in lateral bending.

179 Displacements of the caudal vertebra in relation to the cranial vertebra were calculated
180 from DIC images with a Matlab script. Assuming vertebra to be rigid bodies, the motions
181 (translations and rotations) of each vertebra were computed based on singular value

182 decomposition. The ROM was defined as the relative angle between the vertebra in the
183 sagittal plane between the peak load and unloaded conditions.

184 A pilot study of the load-displacement curves determined that, for porcine spines, the
185 position having a first derivative of 30 N/mm was at the limit of the laxity zone (LZ).
186 Stiffness was defined as the slope of load-displacement relationship in LZ. Although for
187 some specimens this method underestimated the length of the LZ, the stiffness
188 computation was not impacted since it was within the linear region [28].

189 All the computations were performed with dedicated Matlab scripts (Mathworks, Inc.,
190 Natick, MA, USA). All height and strain measurements were evaluated by two
191 independent observers. To limit inter-specimen variability influence, all stiffnesses,
192 heights, and ROMs values were normalized to the intact condition.

193 In addition to posterior disc height, ROM, and stiffness calculations, the true principal
194 strains over the specimen surface (vertebra and IVD) were measured at the peak load.
195 In particular, the disc surface area was manually identified and the minimum, maximum
196 and average of the first and second principal strains were extracted. Those measurements
197 were performed in flexion and extension because the frontal view did not allow
198 consideration of the neuroforamen area.

199 For each parameter, outlying data were preliminarily tested and excluded using the
200 Peirce criterion [29], this resulted in a 10% data exclusion at the maximum. Test
201 parameters were computed based on the sixth cycle. Mean \pm standard deviation of all
202 the outcomes were calculated and presented by group. Due to the small specimen
203 number, comparisons between the three conditions were made for ROM, stiffness,
204 height, and the strain average with a non-parametric test (Wilcoxon's sign rank, with
205 Matlab).

206 **2.8. Cement distribution**

207 In order to study the cement distribution inside of the disc, scans of the specimens have
208 been performed after discoplasty with a clinical computed tomography scanner
209 (Aquilion ONE, Toshiba) with 120 mA, 135 kV and a 0.5 mm voxel. The scans of nine
210 specimens out of ten were available due to a practical mistake. The shape of the cement,
211 its capacity to fill the disc cavity, the endplates and AF contact were visually assessed
212 by a spine surgeon (P.E.) from the 3D reconstruction of the PMMA geometry.
213 Segmentation process was performed in Mimics® image analysis software (Mimics

214 Research, Mimics Innovation Suite v21.0, Materialise, Leuven, Belgium) on the 2D CT
215 images using thresholding algorithm.

216 **3. RESULTS**

217 **3.1. Posterior disc height**

218 The posterior disc height was measured in the three conditions. At peak load, intact
219 posterior disc height was higher in flexion than in extension. Nucleotomy significantly
220 decreased the posterior height for both flexion ($p=0.006$, Wilcoxon) and extension
221 ($p=0.049$, Wilcoxon) (Fig. 3). On the contrary, discoplasty restored the height. Results
222 were normalized to the initial posterior height for each specimen. In extension, height
223 after discoplasty was significantly higher (105% of the intact height) than after
224 nucleotomy (81%) ($p= 0.04$, Wilcoxon). In flexion, posterior disc height was
225 respectively 84% and 94% of the intact height after nucleotomy and discoplasty but the
226 difference between the two conditions was not significant ($p=0.11$, Wilcoxon).

227 **3.2. Range of motion**

228 Intervertebral motions in the applied direction were one order of magnitude higher
229 compared to the other directions. Only the motions in the applied direction are reported
230 here. In flexion and lateral bending, nucleotomy reduced the ROM (Fig. 4). The ROM
231 in extension slightly increased after nucleotomy and discoplasty compared to the intact
232 condition. The results for degenerated and discoplasty discs were normalized by the
233 intact ROM for each motion. ROM was not significantly different between nucleotomy
234 and discoplasty in flexion (Wilcoxon sign-rank test, $p=0.57$), extension ($p=0.43$) and
235 lateral bending ($p=0.50$, Wilcoxon).

236 **3.3. Stiffness**

237 Stiffness was computed for only 9 out of 10 specimens due to a technical problem during
238 acquisition. Specimens had very different behaviours regardless of the loading
239 configuration and spinal level. The majority of the tests presented a “toe-region” before
240 a stiff region. A recovery after discoplasty of the initial behaviour compared to after
241 nucleotomy was also observed (Fig. 5). The results for nucleotomy and discoplasty discs
242 were normalized by the intact stiffness for each loading configuration. Stiffness was not

243 significantly different after nucleotomy and discolplasty in flexion ($p=0.47$, Wilcoxon),
244 extension ($p=0.95$, Wilcoxon) and lateral bending ($p=0.46$, Wilcoxon) (Fig. 6).

245 **3.4. Strain distribution**

246 DIC correlation has been successfully performed in flexion and extension only because
247 the frontal view did not allow all of the disc surface to be captured. First of all, bone
248 strains were in a $[-1.5\%, 1.5\%]$ range on the vertebra surface whereas they reached -17%
249 and $+11\%$ on the discs. Moreover, IVD principal strains presented different behaviours
250 depending on the loading configuration (Fig. 7). In flexion, for all disc conditions, the
251 highest values of compressive strain are located at the cranial and caudal extremities of
252 the IVD, starting from the anterior and spreading toward the posterior along the
253 endplates. After nucleotomy and discolplasty, the trend was more pronounced. However,
254 cemented discs presented lower values in this area than empty discs. The highest values
255 of tensile principal strain were in the centre of the IVD with peak $>3\%$ of strain in the
256 posterior region. In extension, tensile strains were larger in the anterior of the disc while
257 high compressive strains were located in the posterior area of the disc. Discolplasty
258 reduced the strains in most of the disc, whereas for intact and nucleotomy, high strains
259 were found on the whole disc.

260 Nucleotomy seems to have a greater effect on the compressive strain in flexion and
261 extension (Table 1). Meanwhile, discolplasty halved the average tensile strain of disc
262 surface compared to nucleotomy condition in extension ($p=0.0195$, Wilcoxon) but had
263 similar values of second principal strain. Regarding the peak strains, discolplasty only
264 presented a value larger than intact condition for extension. Other extreme strains were
265 observed after nucleotomy although the differences were not significant.

266 **3.5. Cement distribution**

267 Nine specimens have been scanned to control cement distribution within the discs.
268 Visual assessment of the specimen scans focused on the position of the cement mass
269 within the intervertebral disc in the sagittal and frontal planes, whether it was in contact
270 with endplates and AF, the shape of the distribution, and the ratio of disc filling. The
271 majority of specimens had a cement volume located in the posterior of the disc (9/9
272 specimens), centred in the lateral direction (8/9 specimens), in contact with the endplates

273 (8/9). Only two specimens did not present contact between the cement and the AF (Fig.
274 8). The NP cavity was fully filled with cement in 5 specimens, three discs were almost
275 filled at >80% of the NP volume, and one at less than 80%. Among the specimens, seven
276 were validated by a clinician as discoplasty models compared to cement distribution
277 after human surgery taking porcine anatomical specificities into account, and two were
278 sub-optimal (Fig. 9). No outlier corresponded to the sub-optimal cemented specimens.
279 All specimens presented a smaller cement volume than in human surgery (Table 2).

280 **4. DISCUSSION**

281 According to clinical observations [11], a loss of disc height due to disc degeneration
282 would result in a reduction of the neuroforamen where the back nerves are passing,
283 compressing them and creating pain for the patient. This animal *in vitro* study aimed at
284 exploring the feasibility of assessing the mechanical consequences on spine stability
285 after discoplasty surgical procedure. An *in vitro* experiment was successfully conducted
286 to establish posterior disc height, ROM, stiffness, and strains over porcine specimen
287 surfaces.

288 After nucleotomy a decrease of the posterior disc height of 15% was measured. This
289 result validated such *in vitro* nucleotomy as a simulation of degenerated disc.
290 Furthermore, nucleotomy was associated with a decrease of ROM (not statistically
291 significant in our sample). After discoplasty, the injected cement acted like a spacer
292 resulting in a significant recovery of the posterior height (105% of the intact height in
293 extension). This trend supported the clinical observations [11] and confirmed that PCD
294 recovered the disc height and enlarged neuroforamen space, which is the main objective
295 of this surgery. ROM and stiffness did not show any significant difference between the
296 degenerated and treated cases for any loading. Thus, discoplasty did not significantly
297 impact spine flexibility in this experimental setup.

298 To the authors' knowledge, this was the first study addressing the consequences of
299 discoplasty on the distribution of strain on the disc surface. The strain distribution
300 measured after nucleotomy showed a specific pattern with intense regions, while
301 discoplasty reduced this abnormal distribution with more moderate strain values.

302 DIC results showing the AF principal strains can be related to the ROM and the posterior
303 disc height. After nucleotomy, because of the reduced posterior height and because the
304 annulus is no longer constrained from inside, the annulus fibres bulged more, leading to

305 intense tensile strains at the apex of the bulging. At the same time, this more pronounced
306 bulging at mid-height caused a more pronounced concavity at the disc cranial and caudal
307 extremities, which led to larger compressive strains in this region. After discolplasty, the
308 injected cement spaced the endplates, and even if the cement did not stretch radially the
309 disc fibres as the NP would do, the overall bulging was more limited, and less intense
310 tensile strains were measured. As the cement acts as a very stiff spacer, very small strains
311 were visible in most of the disc surface, the only highly strained region in the disc was
312 near the endplates. Strain values after discolplasty did not exceed what the endplates
313 underwent in nucleotomy condition. If the specimen endplates presented any weakness,
314 this could lead to long-term damages due to the load concentration. The peak strain
315 values increased after nucleotomy, and decreased again after cement injection, reaching
316 intact-like values. No correlation between the strain peaks on the specimen surface and
317 the cement distribution assessed from the CT scans was found. Even in the specimens
318 where contact between the AF and the cement was noted, this did not result in a specific
319 strain distribution.

320 The ROM measured at peak load was in the same range as other *in vitro* studies on
321 porcine lumbar spines [22], [30]. Others studies investigating the effect of nucleotomy
322 demonstrated that the absence of NP reduced segmental rotational stability, significantly
323 increasing the ROM [14], [19], [23].

324 Discoplasty being a recent surgical technique, the authors found only one article
325 applying a similar surgery, on dog cervical discs [3]: nucleotomy was also performed
326 through an AF fenestration and a spacer implant was inserted. Similar to the present
327 study, Moissonier *et al* found that nucleotomy completely disrupted spine stability,
328 increasing significantly the ROM. Both the spacer used in their study, and the cement
329 injected in ours failed to recover disc mobility. Similarly, the cement set in the cervical
330 disc by Wilke *et al* reduced the ROM compared to intact disc condition. However, this
331 study tested bone cement to anticipate interbody fusion, and the AF was not fully intact
332 [15]. This was the major difference with soft disc filler materials which are more likely
333 to restore intact ROM as well [14].

334 Although the results were normalized with respect to the intact to integrate the specimen
335 anatomical specificity, and one outlier was removed, inter-specimen variability
336 remained large, with no correlation with the segment level. Our tests differed from most
337 of the literature [28] as the FSUs were tested separately in flexion and extension,
338 therefore direct comparisons of the stiffness are not possible.

339 This study aimed to start exploring the biomechanical effects of discoplasty. Since this
340 is a preliminary study, an animal model was more justifiable for ethical reasons. The
341 use of breed porcine rather than human spines was preferred as they have less inter-
342 specimen variation of anatomy and mechanical properties. Indeed, porcine models are
343 commonly used to replicate human spine surgeries [31], [32]. Porcine spines could be
344 good surrogates for *in vitro* testing, even if they exhibit larger ROM and lower stiffness
345 [33]–[35]. Since the porcine specimens were obtained before reaching skeletal maturity,
346 finding IVDs presenting a similar degenerated level with a vacuum as required for PCD
347 was impossible. Nucleotomy did not aim at modelling a degenerated disc state but at
348 creating the spine instability observed clinically based on the disc vacuum. Porcine
349 results should therefore be qualitatively extrapolated to humans in terms of trends rather
350 than interpreting absolute values as this study aimed at.

351 Vacuum volume has not been measured in this study. The importance of this parameter
352 is unclear in the clinical practice. A recent study investigating the Vacuum Phenomenon
353 (VP) impact for PCD indication concluded that the volume of vacuum could not be used
354 as a proper indication for this surgery [36]. Moreover, during the PCD procedure, the
355 patient position aims at enlarging the intervertebral space by reducing the segmental
356 lordosis. Thus, the volume of the empty disc available during the surgery is larger than
357 the VP computed on imaging.

358 Usual methods to measure the disc height like Farfan or Frobin were not applied here to
359 assess the intervertebral space. Indeed, these methods were conceived for clinical
360 application considering the vertical height along the antero-posterior disc length on
361 medical images, taking account of the whole disc and its orientation. This study,
362 however, focused on the nerve space within the neuroforamen. Only the volume where
363 the nerve passed was critical, based on clinical observations, and the discoplasty surgery
364 was applied in first approach to re-open the foramen space by achieving indirect
365 decompression. That is why a comparative study has been performed selecting two
366 points at the endplates level the closest from the neuroforamen, rather than relying on a
367 more general measurement of the disc height. The study concentrated on parameters
368 with meaning for the clinical purpose of the surgery. Moreover, the most critical case
369 was also investigated: physiologically when the disc is loaded in extension and the
370 neuroforamen is the most reduced. So, measurements at the peak load were more
371 interesting for the study.

372 The impact of AF fenestration during nucleotomy on the segment stability has not been
373 assessed here, however Michalek *et al* reported alterations of IVD mechanics with disc
374 height loss under a compressive load, following different types of incisions [37]. Disc
375 lesions were also found to reduce the peak moment depending on the damage shape [38].
376 As a consequence, our study may overestimate motion range. However, it was
377 hypothesized that the lack of NP would destabilize the segment in larger proportion than
378 the fenestration of AF.

379 Pure moment is the gold-standard loading for *in vitro* spine testing in a relevant bending
380 condition. For spine segments consisting of several vertebrae, bending is usually
381 associated with a follower load equipment to model the *in vivo* kinematics, including the
382 effect of the muscles adding a compressive loading [39], [40]. Similarly, a compressive
383 preload is found in a single FSU, but in this case a follower load cannot be implemented.
384 In this study, an alternative loading configuration was chosen to ensure that reproducible
385 testing conditions could be applied, thus allowing the comparison of the biomechanics
386 of a specimen tested at different times with each of the different disc conditions. The
387 load applied here was a combination of axial compression and bending, an alternative
388 loading to pure bending of the spine [26], [41]–[44]. It has been demonstrated that
389 without preload, *in vivo* stiffness of the spine segment was underestimated applying pure
390 bending [45]. In our study, the combination of axial compression and bending allowed
391 a more physiological spine loading with an axial component which substitutes of the
392 preload.

393 **5. CONCLUSION**

394 So far, the only knowledge about PCD comes from clinical experience on few cases.
395 This paper presents a feasibility study, to develop a test model and perform a preliminary
396 investigation on the biomechanics of PCD. The study also aimed at analyzing and
397 verifying if there is any clear mechanical risk associated with injection of cement in the
398 cavity of a disc. No specific clinical recommendations (e.g. indication for specific
399 patient groups) can be directly obtained from the present study. This study aimed at
400 developing an *in vitro* surrogate to test a highly degenerated disc with vacuum inside,
401 and to assess the biomechanical changes related to discoplasty in porcine spines. The
402 main conclusions could be summarized in key points.

- 403 • The *in vitro* method was successfully developed to model nucleotomy.
- 404 • The *in vitro* testing protocol applied to discoplasty allowed to measure the effect
405 of this minimally invasive surgery on the spine biomechanics.
- 406 • Nucleotomy decreased the posterior disc height. Discoplasty restored the height
407 significantly, maintaining a gap between the vertebral bodies and re-opening the
408 neuroforamen area as observed in clinical practice.
- 409 • The CT scans confirmed that the distribution of the cement had a similar
410 distribution inside the disc for most specimens compared to human post-surgery
411 observations, although the cavity after nucleotomy and the cement volume were
412 smaller than in human cases.
- 413 • Discoplasty did not impact the ROM nor the stiffness, which remained similar
414 to the nucleotomy condition because the cement did not directly interact with the
415 AF nor the facets.
- 416 • Discoplasty concentrated the strains along the endplates, reducing the strain
417 value on the middle of the disc. The average strain over the disc was decreased
418 after discoplasty compared to nucleotomy, limiting the risks of fibre tears.
- 419 • The goal of this preliminary study on a limited number of porcine specimens was
420 to establish trends which could justify a larger study on human specimens.

421 **Acknowledgments**

422 The Authors wish to thank Federico Morosato from the University of Bologna for
423 providing the Matlab scripts.

424 Villalba Hospital is acknowledged for hosting the scan sessions; special thanks to
425 Pierangela Moro for the skilled advice and for her great patience.

426 Special thanks are expressed to Cameron James, ESR within the Spinner project, for
427 proof-reading the manuscript.

428 The use Mimics Software was possible thanks to the Hungarian Scientific Research
429 Fund (OTKA FK123884).

430 This project was founded by European Union's Horizon 2020 Marie Skłodowska-Curie
431 ITN grant SPINNER No. 766012.

432 **Conflict of interest statement**

433 There is no potential conflict of interest: none of the Authors received or will receive
434 direct or indirect benefits from third parties for the performance of this study.

435

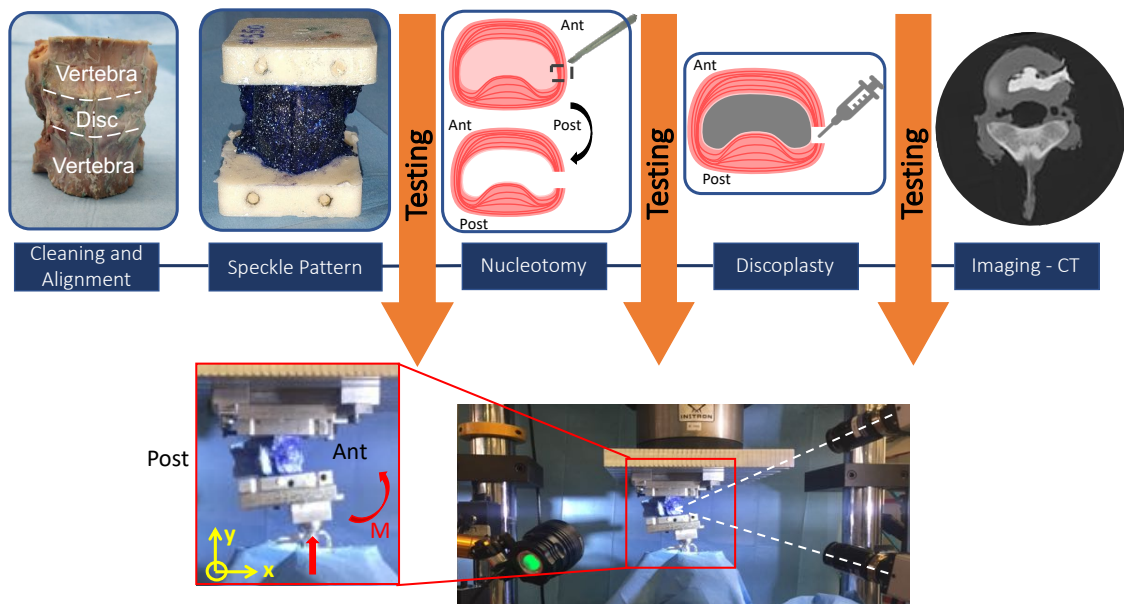
- 437 [1] « 6. Priority diseases and reasons for inclusion », in *WHO | Priority Medicines*
438 *for Europe and the World Update Report*, 2013.
- 439 [2] I. Oda, K. Abumi, B.-S. Yu, H. Sudo, et A. Minami, « Types of Spinal Instability
440 That Require Interbody Support in Posterior Lumbar Reconstruction: An In Vitro
441 Biomechanical Investigation. [Miscellaneous Article] », *Spine*, vol. 28, n° 14, p.
442 1573-1580, juill. 2003.
- 443 [3] P. Moissonnier, L. Desquilbet, D. Fitzpatrick, et F. Bernard, « Radiography and
444 biomechanics of sixth and seventh cervical vertebrae segments after disc
445 fenestration and after insertion of an intervertebral body spacer », *Vet. Comp.*
446 *Orthop. Traumatol.*, vol. 27, n° 1, p. 54-61, 2014, doi: 10.3415/VCOT-11-11-
447 0159.
- 448 [4] X. Li, Y. Song, et H. Duan, « Reconstruction of Segmental Stability of Goat
449 Cervical Spine with Poly (D, L-lactic acid) Cage », *Orthop. Surg.*, vol. 7, n° 3, p.
450 266-272, 2015, doi: 10.1111/os.12192.
- 451 [5] F. Kandziora, R. Pflugmacher, M. Scholz, T. D. Eindorf, K. J. Schnake, et N. P.
452 Haas, « Bioabsorbable Interbody Cages in a Sheep Cervical Spine Fusion
453 Model. », *Spine*, vol. 29, n° 17, p. 1845-1855, sept. 2004.
- 454 [6] F. Kandziora *et al.*, « Comparison of BMP-2 and combined IGF-I/TGF- β 1
455 application in a sheep cervical spine fusion model », *Eur. Spine J.*, vol. 11, n° 5,
456 p. 482-493, oct. 2002, doi: 10.1007/s00586-001-0384-4.
- 457 [7] Y. Gu, Z. Yao, L. Jia, J. Qi, et J. Wang, « In vivo experimental study of hat type
458 cervical intervertebral fusion cage (HCIFC) », *Int. Orthop.*, vol. 34, n° 8, p.
459 1251-1259, déc. 2010, doi: 10.1007/s00264-010-0978-8.
- 460 [8] Z. Chunguang *et al.*, « Evaluation of Bioabsorbable Multiamino Acid
461 Copolymer/ α -Tri-Calcium Phosphate Interbody Fusion Cages in a Goat Model »,
462 *Spine*, vol. 36, n° 25, p. E1615-E1622, déc. 2011, doi:
463 10.1097/BRS.0b013e318210ca32.
- 464 [9] M. J. Allen, Y. Hai, N. R. Ordway, C.-K. Park, B. Bai, et H. A. Yuan,
465 « Assessment of a synthetic anterior cervical ligament in a spinal fusion model in
466 sheep », *Spine J.*, vol. 2, n° 4, p. 261-266, juill. 2002, doi: 10.1016/S1529-
467 9430(02)00188-2.
- 468 [10] S. E. Emery, D. A. Fuller, et S. D. Stevenson, « Ceramic Anterior Spinal Fusion:
469 Biologic and Biomechanical Comparison in a Canine Model. [Miscellaneous
470 Article] », *Spine*, vol. 21, n° 23, p. 2713-2719, déc. 1996.
- 471 [11] P. P. Varga, G. Jakab, I. B. Bors, A. Lazary, et Z. Szövérfi, « Experiences with
472 PMMA cement as a stand-alone intervertebral spacer », *Orthop.*, vol. 44, n° 1, p.
473 1-8, nov. 2015, doi: 10.1007/s00132-014-3060-1.
- 474 [12] C. Sola *et al.*, « Percutaneous cement discoplasty for the treatment of advanced
475 degenerative disk disease in elderly patients », *Eur. Spine J.*, mars 2018, doi:
476 10.1007/s00586-018-5547-7.
- 477 [13] L. Kiss, P. P. Varga, Z. Szoverfi, G. Jakab, P. E. Eltes, et A. Lazary, « Indirect
478 foraminal decompression and improvement in the lumbar alignment after
479 percutaneous cement discoplasty », *Eur. Spine J.*, avr. 2019, doi:
480 10.1007/s00586-019-05966-7.
- 481 [14] H.-J. Wilke, F. Heuer, C. Neidlinger-Wilke, et L. Claes, « Is a collagen scaffold
482 for a tissue engineered nucleus replacement capable of restoring disc height and
483 stability in an animal model? », *Eur. Spine J.*, vol. 15, n° 3, p. 433-438, août
484 2006, doi: 10.1007/s00586-006-0177-x.

- 485 [15] H.-J. Wilke, A. Kettler, et L. Claes, « Primary stabilizing effect of interbody
486 fusion devices for the cervical spine: an in vitro comparison between three
487 different cage types and bone cement », *Eur. Spine J.*, vol. 9, n° 5, p. 410-416,
488 oct. 2000, doi: 10.1007/s005860000168.
- 489 [16] G. Vadalà *et al.*, « A Nucleotomy Model with Intact Annulus Fibrosus to Test
490 Intervertebral Disc Regeneration Strategies », *Tissue Eng. Part C Methods*, vol.
491 21, n° 11, p. 1117-1124, 2015, doi: <http://dx.doi.org/10.1089/ten.tec.2015.0086>.
- 492 [17] G. Vadalà *et al.*, « The Transpedicular Approach As an Alternative Route for
493 Intervertebral Disc Regeneration »:, *Spine*, vol. 38, n° 6, p. E319-E324, mars
494 2013, doi: 10.1097/BRS.0b013e318285bc4a.
- 495 [18] M. Shea, T. Y. Takeuchi, R. H. Wittenberg, A. A. White, et W. C. Hayes, « A
496 Comparison of the Effects of Automated Percutaneous Discectomy and
497 Conventional Discectomy on Intradiscal Pressure, Disk Geometry, and
498 Stiffness »:, *J. Spinal Disord.*, vol. 7, n° 4, p. 317-325, août 1994, doi:
499 10.1097/00002517-199408000-00005.
- 500 [19] W. Johannessen, J. M. Cloyd, G. D. O'Connell, E. J. Vresilovic, et D. M. Elliott,
501 « Trans-Endplate Nucleotomy Increases Deformation and Creep Response in
502 Axial Loading », *Ann. Biomed. Eng.*, vol. 34, n° 4, p. 687-696, avr. 2006, doi:
503 10.1007/s10439-005-9070-8.
- 504 [20] J. S. Tan et S. Uppuganti, « Cumulative Multiple Freeze-Thaw Cycles and
505 Testing Does Not Affect Subsequent Within-Day Variation in Intervertebral
506 Flexibility of Human Cadaveric Lumbosacral Spine », *SPINE*, vol. 37, n° 20, p.
507 E1238-E1242, 2012.
- 508 [21] J. M. Cottrell, M. C. H. van der Meulen, J. M. Lane, et E. R. Myers, « Assessing
509 the Stiffness of Spinal Fusion in Animal Models », *HSS J.*, vol. 2, n° 1, p. 12-18,
510 févr. 2006, doi: 10.1007/s11420-005-5123-7.
- 511 [22] J. P. Dickey et D. J. Kerr, « Effect of specimen length: are the mechanics of
512 individual motion segments comparable in functional spinal units and
513 multisegment specimens? », *Med. Eng. Phys.*, vol. 25, n° 3, p. 221-227, avr.
514 2003, doi: 10.1016/S1350-4533(02)00152-2.
- 515 [23] F. Russo *et al.*, « Biomechanical Evaluation of Transpedicular Nucleotomy With
516 Intact Annulus Fibrosus »:, *SPINE*, vol. 42, n° 4, p. E193-E201, févr. 2017, doi:
517 10.1097/BRS.0000000000001762.
- 518 [24] D. J. Sucato, « Thoracoscopic Discectomy and Fusion in an Animal Model: Safe
519 and Effective When Segmental Blood Vessels Are Spared. », *SPINE*, vol. 27, n°
520 8, p. 880-886, 2002.
- 521 [25] Chung et Teoh, « Multi-axial Spine Biomechanical Testing System with Speckle
522 Displacement Instrumentation », *J. Biomech. Eng.*, vol. 124, n° 4, p. 471-477,
523 août 2002, doi: 10.1115/1.1493803.
- 524 [26] M. Palanca, M. Marco, M. L. Ruspi, et L. Cristofolini, « Full-field strain
525 distribution in multi-vertebra spine segments: An in vitro application of digital
526 image correlation », *Med. Eng. Phys.*, vol. 52, p. 76-83, févr. 2018, doi:
527 10.1016/j.medengphy.2017.11.003.
- 528 [27] M. Palanca, T. M. Brugo, et L. Cristofolini, « USE OF DIGITAL IMAGE
529 CORRELATION TO INVESTIGATE THE BIOMECHANICS OF THE
530 VERTEBRA », *J. Mech. Med. Biol.*, vol. 15, n° 02, p. 1540004, avr. 2015, doi:
531 10.1142/S0219519415400047.
- 532 [28] H.-J. Wilke, K. Wenger, et L. Claes, « Testing criteria for spinal implants:
533 recommendations for the standardization of in vitro stability testing of spinal

- 534 implants », *Eur. Spine J.*, vol. 7, n° 2, p. 148-154, mai 1998, doi:
535 10.1007/s005860050045.
- 536 [29] S. M. Ross, « Peirce's criterion for the elimination of suspect experimental
537 data », *J. Eng. Technol.*, p. 1-12, 2003.
- 538 [30] J. T. Lysack, J. P. Dickey, G. A. Dumas, et D. Yen, « A continuous pure moment
539 loading apparatus for biomechanical testing of multi-segment spine specimens »,
540 *J. Biomech.*, vol. 33, n° 6, p. 765-770, juin 2000, doi: 10.1016/S0021-
541 9290(00)00021-X.
- 542 [31] Busscher, « Comparative anatomical dimensions of the complete human and
543 porcine spine », 2010.
- 544 [32] C. Daly, P. Ghosh, G. Jenkin, D. Oehme, et T. Goldschlager, « A Review of
545 Animal Models of Intervertebral Disc Degeneration: Pathophysiology,
546 Regeneration, and Translation to the Clinic », *BioMed Res. Int.*, vol. 2016, 2016,
547 doi: 10.1155/2016/5952165.
- 548 [33] H.-J. Wilke, J. Geppert, et A. Kienle, « Biomechanical in vitro evaluation of the
549 complete porcine spine in comparison with data of the human spine », *Eur. Spine
550 J.*, vol. 20, n° 11, p. 1859-1868, nov. 2011, doi: 10.1007/s00586-011-1822-6.
- 551 [34] J. P. Dickey, G. A. Dumas, et D. A. Bednar, « Comparison of porcine and human
552 lumbar spine flexion mechanics* », *Vet. Comp. Orthop. Traumatol.*, vol. 16, n°
553 01, p. 44-49, 2003, doi: 10.1055/s-0038-1632753.
- 554 [35] I. Busscher, A. J. van der Veen, J. H. van Dieen, I. Kingma, G. J. Verkerke, et A.
555 G. Veldhuizen, « In Vitro Biomechanical Characteristics of the Spine A
556 Comparison Between Human and Porcine Spinal Segments », *SPINE*, vol. 35, n°
557 2, p. E35-E42, janv. 2010, doi: 10.1097/BRS.0b013e3181b21885.
- 558 [36] G. Camino Willhuber *et al.*, « Development of a New Therapy-Oriented
559 Classification of Intervertebral Vacuum Phenomenon With Evaluation of Intra-
560 and Interobserver Reliabilities », *Glob. Spine J.*, p. 2192568220913006, mars
561 2020, doi: 10.1177/2192568220913006.
- 562 [37] A. J. Michalek et J. C. Iatridis, « Height and torsional stiffness are most sensitive
563 to annular injury in large animal intervertebral discs », *Spine J.*, vol. 12, n° 5, p.
564 425-432, mai 2012, doi: 10.1016/j.spinee.2012.04.001.
- 565 [38] R. E. Thompson, M. J. Percy, et T. M. Barker, « The mechanical effects of
566 intervertebral disc lesions », *Clin. Biomech.*, vol. 19, n° 5, p. 448-455, juin 2004,
567 doi: 10.1016/j.clinbiomech.2004.01.012.
- 568 [39] A. G. Patwardhan, R. M. Havey, K. P. Meade, B. Lee, et B. Dunlap, « A
569 Follower Load Increases the Load-Carrying Capacity of the Lumbar Spine in
570 Compression. », *SPINE*, vol. 24, n° 10, p. 1003-1009, 1999.
- 571 [40] A. G. Patwardhan, K. P. Meade, et B. Lee, « A Frontal Plane Model of the
572 Lumbar Spine Subjected to a Follower Load: Implications for the Role of
573 Muscles », *J. Biomech. Eng.*, vol. 123, n° 3, p. 212-217, juin 2001, doi:
574 10.1115/1.1372699.
- 575 [41] M. A. Adams, S. May, B. J. C. Freeman, H. P. Morrison, et P. Dolan, « Effects of
576 Backward Bending on Lumbar Intervertebral Discs: Relevance to Physical
577 Therapy Treatments for Low Back Pain. », *SPINE*, vol. 25, n° 4, p. 431-437,
578 2000.
- 579 [42] M. Al-Rawahi, J. Luo, P. Pollintine, P. Dolan, et M. A. Adams, « Mechanical
580 Function of Vertebral Body Osteophytes, as Revealed by Experiments on
581 Cadaveric Spines »:, *Spine*, vol. 36, n° 10, p. 770-777, mai 2011, doi:
582 10.1097/BRS.0b013e3181df1a70.

- 583 [43] M. L. Ruspi, M. Palanca, C. Faldini, et L. Cristofolini, « Full-field in vitro
584 investigation of hard and soft tissue strain in the spine by means of Digital Image
585 Correlation », *Muscles Ligaments Tendons J.*, vol. 7, n° 4, p. 538-545, avr. 2018,
586 doi: 10.11138/mltj/2017.7.4.538.
- 587 [44] M. Adams et P. Dolan, « Time-dependent changes in the lumbar spine's
588 resistancce to bending », *Clin. Biomech.*, vol. 11, n° 4, p. 194-200, juin 1996, doi:
589 10.1016/0268-0033(96)00002-2.
- 590 [45] M. G. Gardner-Morse et I. A. Stokes, « Physiological axial compressive preloads
591 increase motion segment stiffness, linearity and hysteresis in all six degrees of
592 freedom for small displacements about the neutral posture », *J. Orthop. Res.*, vol.
593 21, n° 3, p. 547-552, janv. 2003, doi: 10.1016/S0736-0266(02)00199-7.
594
595

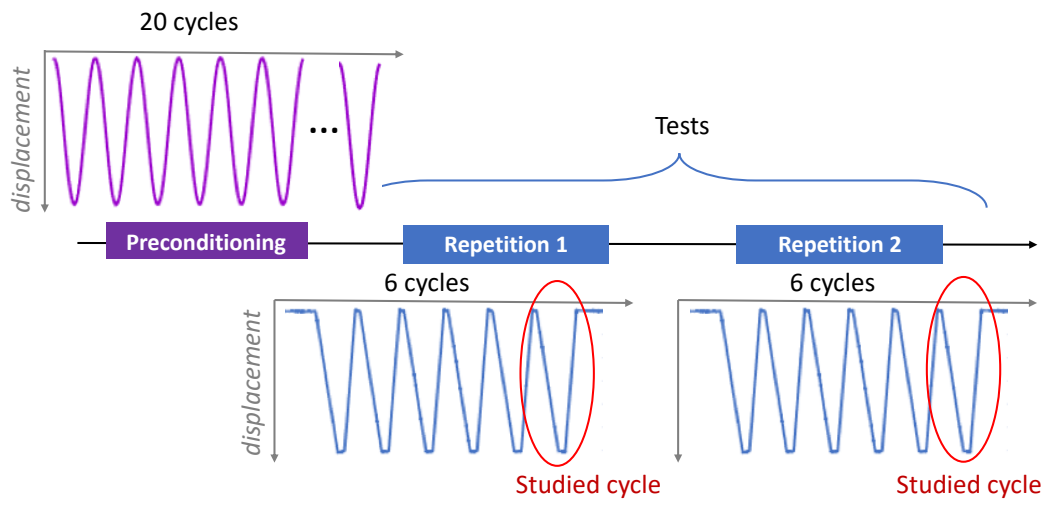
596 CAPTIONS TO FIGURES



597
598
599

Fig. 1 – Experimental workflow of the study. The arrow represents the applied load and the resulting moment M .

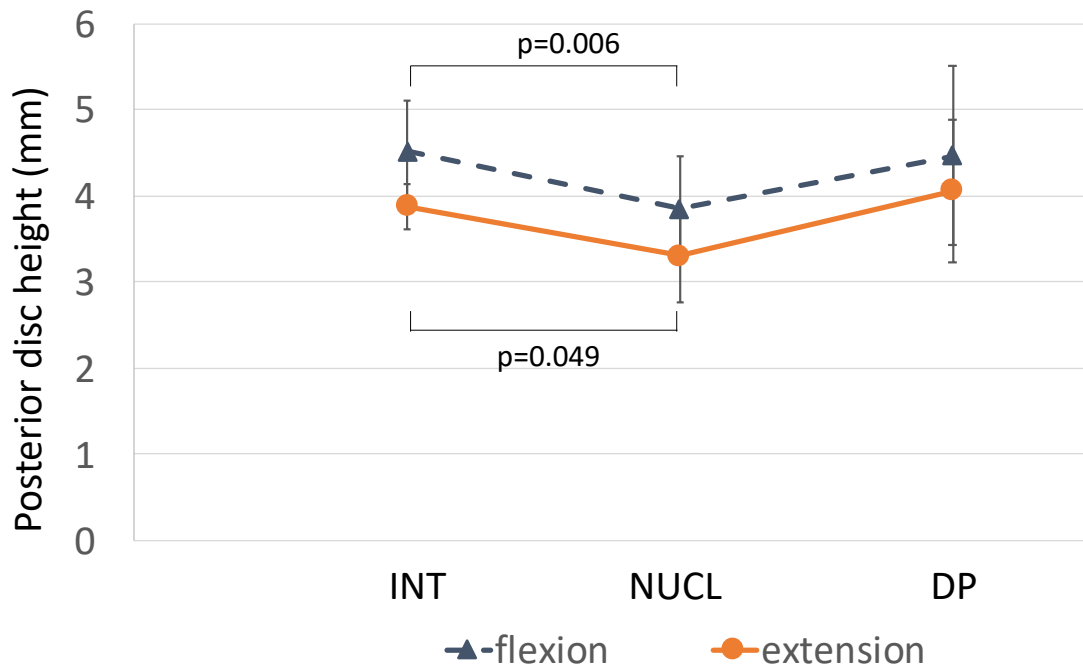
600



601

602 **Fig. 2** – Workflow of the applied displacement for flexion, extension, and lateral
603 bending.

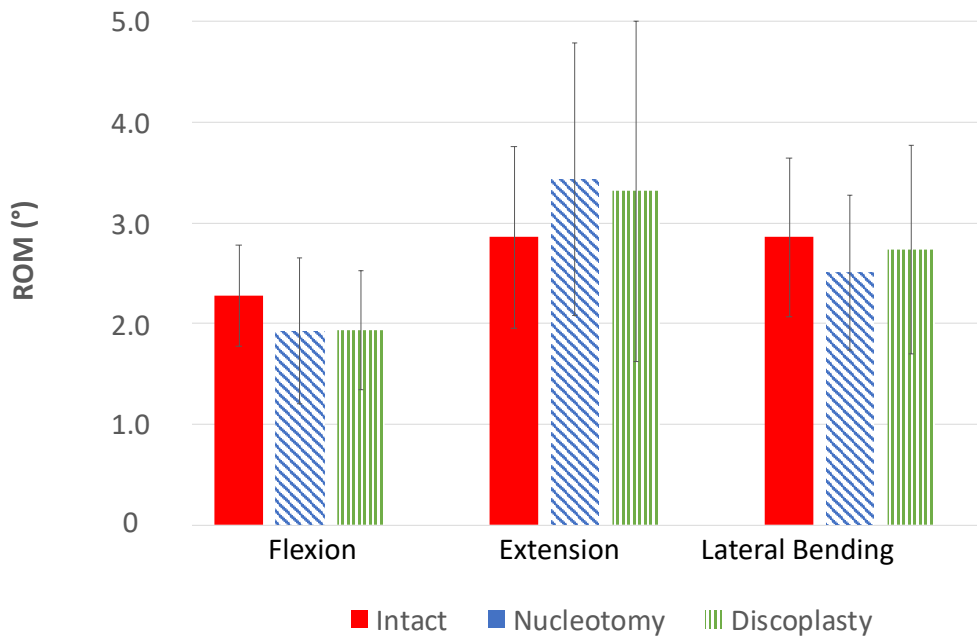
604



605

606 **Fig. 3** – Intervertebral posterior disc height recorded at the peak load in intact
607 condition, after nucleotomy, and discoplasty for both motions. Average over all
608 specimens and standard deviation were represented (n=10). Normalized data showed
609 significant differences in flexion (p=0.11) and extension (p=0.04) between NUCL and
610 DP.

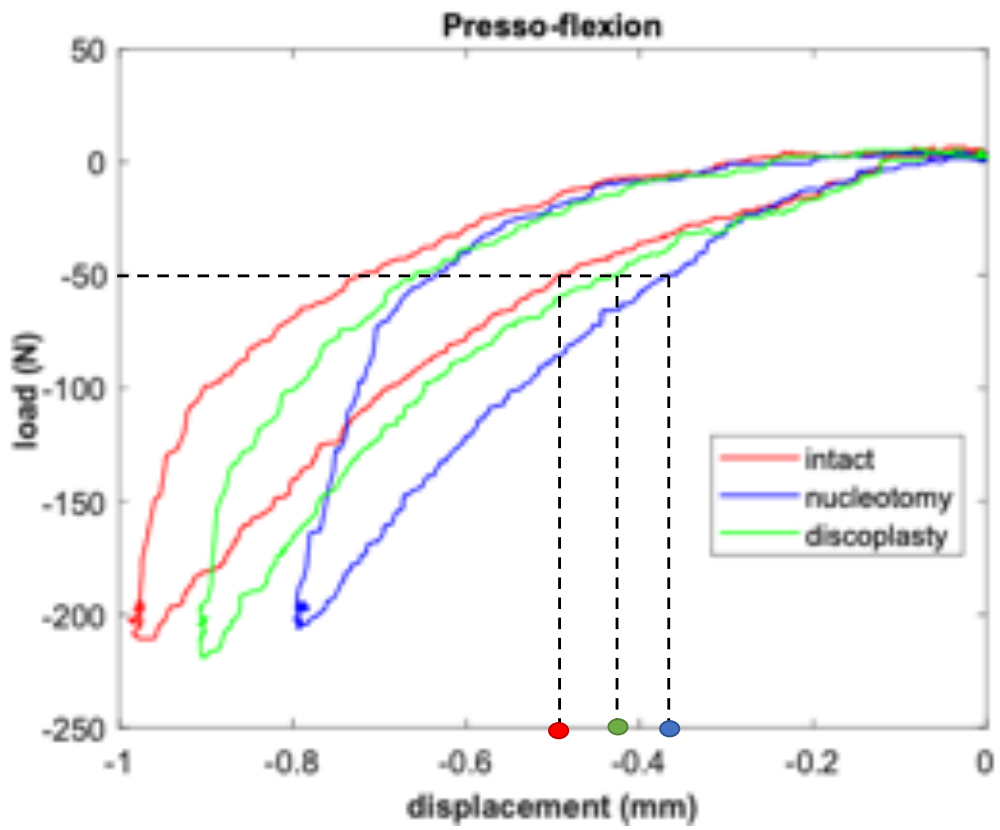
611



612

613 **Fig. 4** – Range of Motion recorded at peak load for flexion, extension and lateral
614 bending, in all disc conditions. Normalized data were not statistically significant
615 ($p>0.1$).

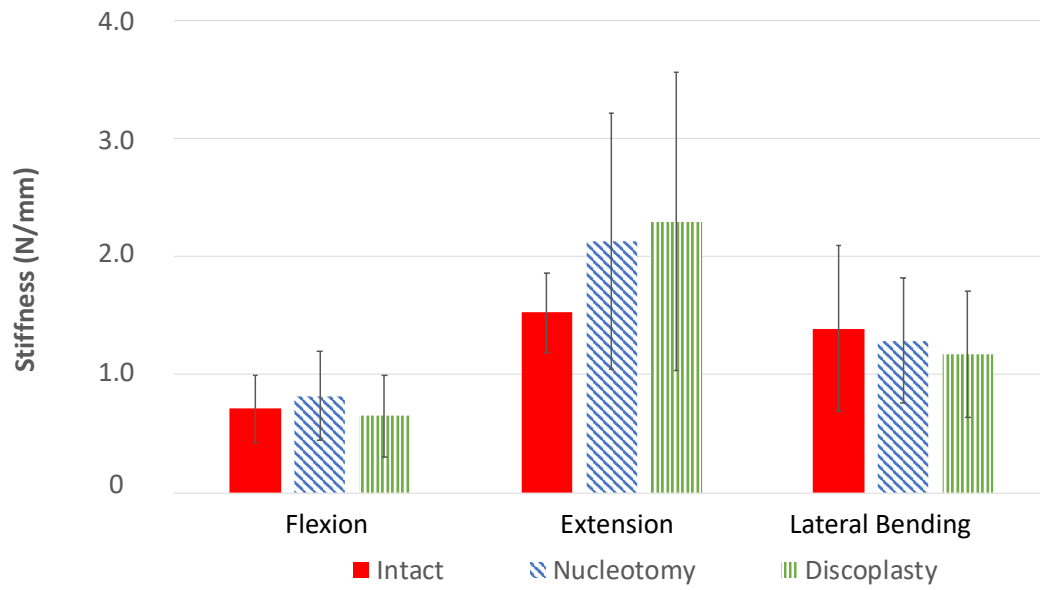
616



617

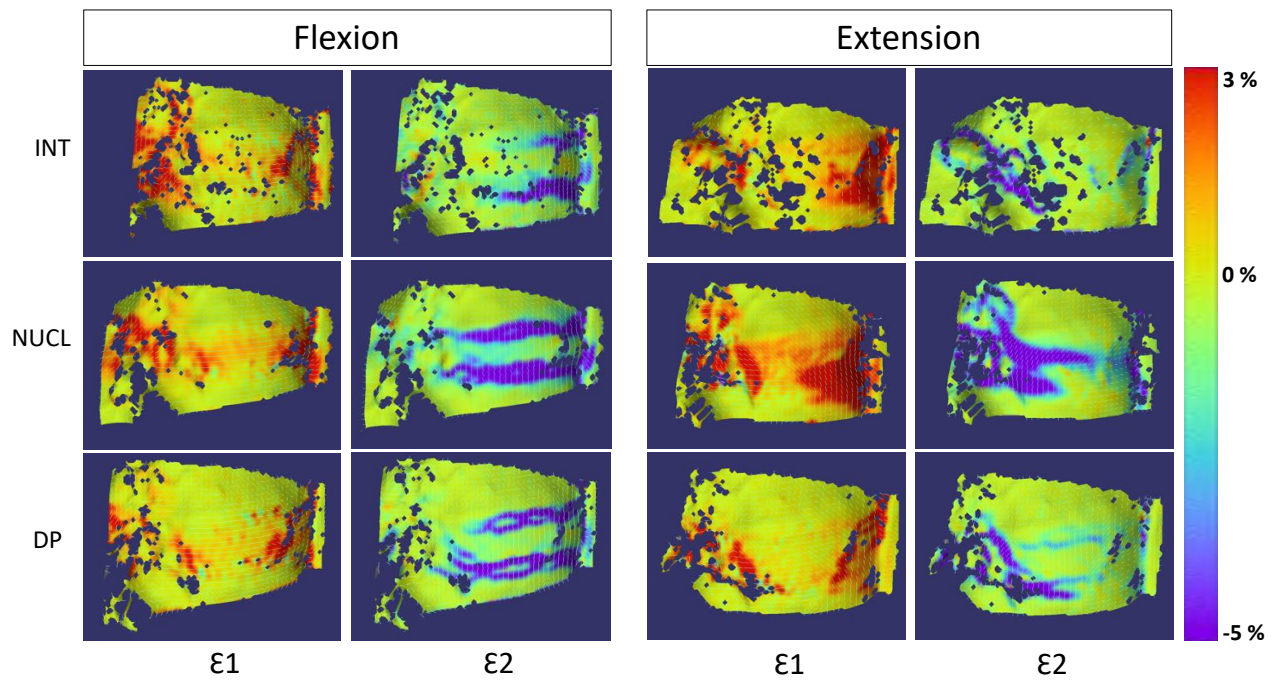
618 **Fig. 5** – Load-displacement curve of a representative specimen tested in extension in
619 all disc conditions.

620



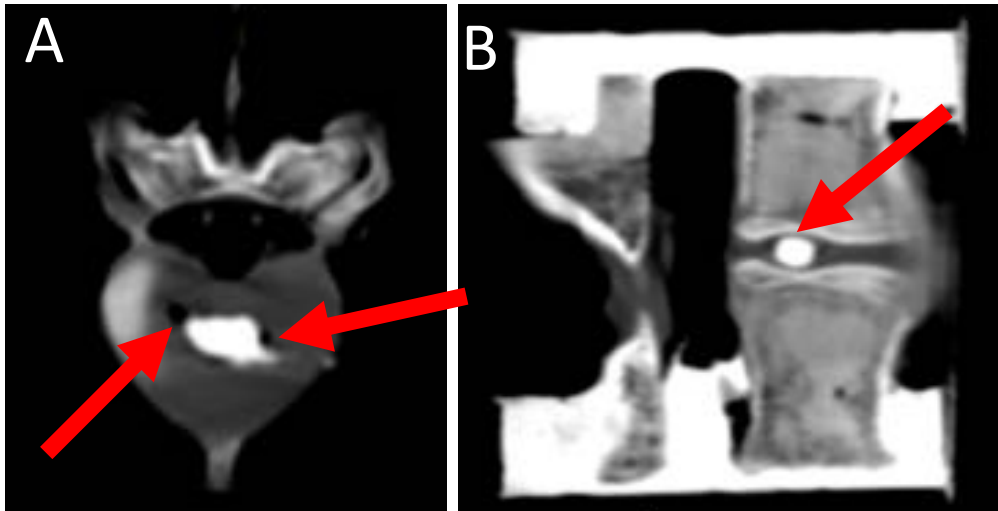
621

622 **Fig. 6** – Stiffness results in all conditions for all loading configurations. Average was
623 done over all specimens. Normalized data were not statistically significant ($p>0.1$).



625

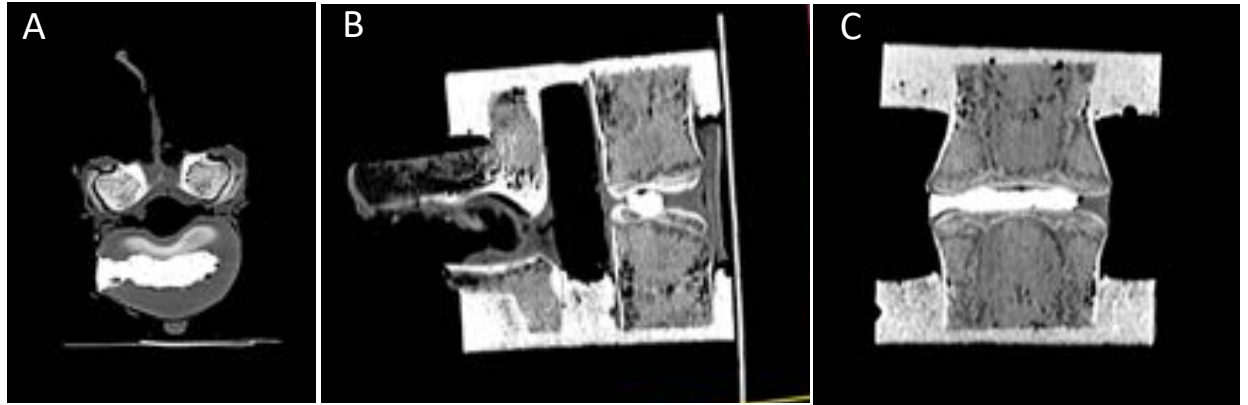
626 **Fig. 7** – Showed a typical strain distribution over a specimen surface for a flexion (left)
 627 and extension (right) bending with first and second principal strains represented for
 628 each motion.



629

630

631 **Fig. 8** –Sub optimal cement distribution. CT scans of porcine specimens in axial (A)
632 and sagittal (B) planes. PMMA did not reach the annulus and the endplates (arrows),
633 leaving vacuum.
634



635

636 **Fig. 9** – Ideal distribution of the PMMA in the porcine model. CT scan of the porcine
637 specimen, A (axial plane) the PMMA filled out the empty space after nucleotomy, B
638 (sagittal plane) and C (coronal plane) the PMMA reached the two endplates and adapted
639 to the geometry.

640 **TABLES**

641 *Table 1: Principal strains recorded over the disc surface in Flexion and Extension: The*
 642 *mean and peak (of 10 specimens) are reported for ϵ_1 and for ϵ_2 .*

ϵ_1	Flexion		Extension	
	Mean (%)	Peak (%)	Mean (%)	Peak (%)
Intact	1.3±0.6	7.5±2.8	2.2±1.0	11.7±6.0
Nucleotomy	1.3±0.7	10.5±7.1	1.9±0.6	10.1±3.9
Discoplasty	1.0±0.5	8.7±3.5	1.2±0.7	10.0±4.1

643

ϵ_2	Flexion		Extension	
	Mean (%)	Peak (%)	Mean (%)	Peak (%)
Intact	-2.0±1.2	-17.2±6.1	-0.5±0.4	-8.2±7.5
Nucleotomy	-2.8±1.6	-18.7±8.9	-1.7±1.5	-12.5±10.4
Discoplasty	-1.7±0.9	-16.5±7.3	-0.7±0.8	-13.3±5.3

644

645 *Table 2: Surface area and volume of the injected cement after segmentation.*

646

Specimen	Spine level	Cement surface area (mm²)	Cement volume (mm³)
#1	T13-L1*	257.8	282.8
#2	L3-L4	465.8	476.7
#3	T13-L1*	211.6	143.5
#4	L5-L6	623.7	673.9
#5	T13-L1*	712.3	750.3
#6	L3-L4	552.0	608.7
#7	L3-L4	742.2	776.5
#8	L3-L4	557.6	505.4
#9	T15-L1*	592.7	685.0
Mean (SD)	-	524.0 (184.2)	544.8 (215.7)

647 * *Porcine spines have a variable number of thoracic vertebrae (between 13 and 15).*